Monatshefte für Chemie 131, 1267–1280 (2000)

Monatshefte für Chemie
Chemical Monthly

Synthesis, Characterization, and Fluxional Behaviour of Binuclear Palladium Complexes with a Half-A-Frame Structure

Felipe Gómez-de la Torre[1], **Yolanda Gutiérrez**[1], **Félix A. Jalón**[1,*], **Blanca R. Manzano**[1], and **Ana Rodríguez**[2]

[1] Departamento de Química Inorgánica, Orgánica y Bioquímica, Universidad de Castilla-La Mancha, Facultad de Químicas, E-13071 Ciudad Real, Spain
[2] Escuela Técnica Superior de Ingeniería Industrial, E-13071 Ciudad Real, Spain

Summary. Partial removal of chloride anions from the dimer $[Pd(\eta^3\text{-}2\text{-}CH_3\text{–}C_3H_4)(\mu\text{-}Cl)]_2$ with $AgTf$ ($Tf = CF_3SO_3$) followed by addition of *dppm* affords $[Pd_2(\eta^3\text{-}Me\text{–}C_3H_4)_2(\mu\text{-}Cl)(\mu\text{-}dppm)]Tf$ (**1**). The substitution of Cl^- by X^- ($X = pz$, SC_6F_5, S_{py}) using the appropriate salts yields the new derivatives $[Pd_2(\eta^3\text{-}Me\text{–}C_3H_4)_2(\mu\text{-}X)(\mu\text{-}dppm)]Tf$ (**2**–**4**). All complexes exhibit a dinuclear half-A-frame structure with two isomers present in solution. The isomers differ in the relative orientation of the two allyl groups (*cis* or *trans*). The isomer interconversion was studied by variable temperature ^1H NMR spectroscopy. The molecular structures of **2** and **4** were solved by X-ray diffraction studies. A distorted boat conformation of the seven- or six-membered metallacycle was found in both cases.

Keywords. Organometallics; Palladium; Binuclear compounds; Allyl; Fluxional behaviour.

Introduction

Binuclear Pd and Pt complexes with two *dppm* (*bis*-(diphenylphosphino)-methane) bridging ligands are known in structures of type **A**, **B**, and **C** [1] (Scheme 1). Compounds of type **B** are known as A-frame complexes, and their preparation usually involves addition of unsaturated ligands such as alkynes [2], SO_2 [3], CO [4], *R*CN [4, 5], and ArNN derivatives [6] to the *M-M* bond of type **A** compounds or, alternatively, a three-fragment oxidative addition to two-centre palladium(0) compounds [4, 7]. Homobridged binuclear complexes of type **C** are prepared by dimerization of mononuclear Pd(II) compounds [8]. Hetero-bridged compounds of type **D** retain half of the molecular backbone of an A-frame complex and are hardly found in Pd chemistry. In the work described here we prepared monocationic complexes of structural type **D** where the *Y* and *L* groups have been replaced by a η^3-2-CH_3–C_3H_4 ligand bonded to each palladium atom. This type of half-A-frame compound offers the possibility of studying the fluxional behaviour of an allyl group coordinated to a Pd centre in an asymmetric environment created by two

* Corresponding author

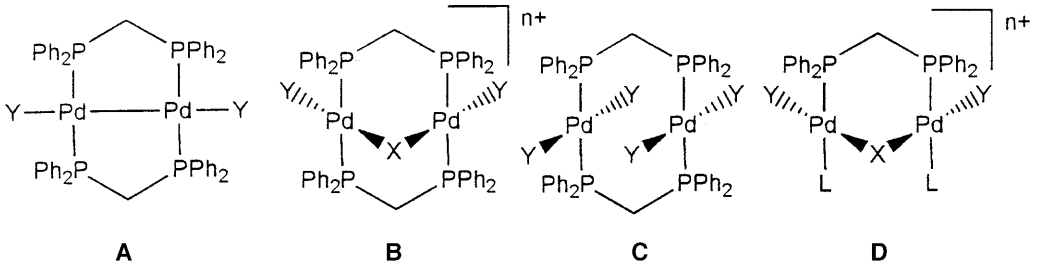

Scheme 1

different ancillary ligands, *X* and *dppm*, in a stable metallacycle. In addition, the influence of the three-electron donor ligand *X* in this metallacycle on the dynamic behaviour of the allyl moiety has been studied in a series of complexes of similar structure.

Results and Discussion

Synthesis of complexes

The partial removal of chloride anions from the dimer $[Pd(\eta^3\text{-}2\text{-}CH_3\text{–}C_3H_4)(\mu\text{-}Cl)]_2$ with 1 equivalent of silver triflate in acetone and the addition of 1 equivalent of *dppm* affords $[Pd_2(\eta^3\text{-}Me\text{–}C_3H_4)_2(\mu\text{-}Cl)(\mu\text{-}dppm)]Tf$ ($Tf = CF_3SO_3$, **1**) according to

$$[Pd(\eta^3\text{-}2\text{-}Me\text{-}C_3H_4)(\mu\text{-}Cl)]_2 + AgTf + dppm \longrightarrow [Pd_2(\eta^3\text{-}2\text{-}Me\text{-}C_3H_4)_2(\mu\text{-}Cl)(\mu\text{-}dppm)]Tf + AgCl$$

1 is an excellent starting material for the synthesis of new hetero-bridged complexes of the formula $[Pd_2(\eta^3\text{-}2\text{-}Me\text{-}C_3H_4)_2(\mu\text{-}X)(\mu\text{-}dppm)]Tf$ ($X^- =$ N,N-pyrazolate (*pz*, **2**), 2-pentafluorophenylthiolate (SC_6F_5, **3**), pyridine-2-thiolate (S*py*, **4**)). Compounds **2–4** can be obtained by reaction of **1** with 1 equivalent of the corresponding sodium, thallium, or potassium salt of X^- in acetone or *THF* according to the following equation:

$$[Pd_2(\eta^3\text{-}2\text{-}Me\text{-}C_3H_4)_2(\mu\text{-}Cl)(\mu\text{-}dppm)]Tf + QX \longrightarrow [Pd_2(\eta^3\text{-}2\text{-}Me\text{-}C_3H_4)_2(\mu\text{-}X)(\mu\text{-}dppm)]Tf + QCl$$

$$(Q = Na,\ X = pz\ (\mathbf{2});\ Q = Tl,\ X = SC_6F_5\ (\mathbf{3});\ Q = K,\ X = Spy\ (\mathbf{4}))$$

Complexes **1–4** are stable at air in the solid state and under a nitrogen atmosphere in solution.

Spectroscopic characterization

Compounds **1–4** were characterized by elemental analysis, as well as by IR, ^1H, $^{31}P\{^1H\}$, and $^{13}C\{^1H\}$ NMR (also ^{19}F NMR for **3**), and mass spectroscopy (**3**). An X-ray crystallography study was also performed for **2** and **4** (see below). In the IR spectra, characteristic vibrations for the allyl, *dppm*, and *X* ligands as well as for the Tf^- anion can be observed. The most significant data are collected in the

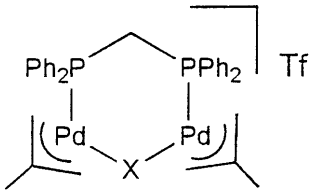

Scheme 2

Experimental section. The absorptions at 228 and 250 cm^{-1} for ν(Pd–Cl) in complex **1** are indicative of a bridging function of this group [9]. In the mass spectra (FAB^+) of **3** a peak is observed at 907 Daltons corresponding to $[Pd_2(C_4H_7)_2(dppm)(SC_6F_5)]^+$. The isotopic distribution is that expected for a fragment with the formula $C_{39}H_{36}F_5P_2SPd_2$. From all these data, the most reasonable structure for these derivatives consists of two allyl-Pd units doubly bridged by the *dppm* and *X* groups to complete the square planar geometry around the Pd atom (see Scheme 2).

Two broad singlets of nearly identical intensity are observed in the $^{31}P\{^1H\}$ NMR spectra of **1–3** at room temperature in acetone-d_6, whereas only one sharp signal is observed for **4**. However, at −60°C two different sharp singlets are observed even for **4**. All ^{31}P signals appear in a narrow range of chemical shifts for the whole set of compounds (16–26 ppm). These chemical shifts are characteristic of a μ-P_2-*dppm* coordination in Pd(II) dinuclear compounds [2g, 7a]. Accordingly, **1–4** may be present in two isomeric forms with the *dppm* moiety in a symmetric environment. A fluxional process would interconvert the two isomers and give rise to the broadening of the signals for **1–3** and the existence of only one averaged resonance for **4** at room temperature.

The ^1H and $^{13}C\{^1H\}$ NMR spectra support the hypothesis outlined above. The corresponding data for the allyl and *dppm* ligands are compiled in Tables 1 (^1H) and 2 (^{13}C). The data for the corresponding bridging *X* ligands can be found in the Experimental section.

The ^1H NMR spectra show very broad signals for **2–4** at room temperature. The recording temperature to assign the different resonances specified in Tables 1 was chosen in order to improve the resolution and allow the most complete assignment of the spectra. Two types of asymmetric allylic groups, with four different allylic protons each, are observed in a quite similar ratio (see Table 1). As previously observed for allyl ligands [10], the CH_2 allylic groups *trans* to phosphorus are deshielded with respect to the analogous *cis* groups both in the ^1H and $^{13}C\{^1H\}$ NMR spectra. In addition, coupling with phosphorus (verified by ^{31}P decoupling) makes the resonances for the *trans* CH_2 groups more complex as a consequence of the magnetic inequivalence of the two P atoms in the molecule. In some cases, an apparent coupling constant can be measured in the spectra (see Tables 1 and 2), and this is always bigger for H_{anti} than for H_{syn}; the coupling H_{syn}-$H_{syn'}$ is also observed.

From the ^1H NMR data for the allylic units one can consider two possibilities: (*i*) one isomer with two inequivalent asymmetric allylic groups or (*ii*) two isomers with equivalent asymmetric groups. The fact that the integrals for the two allylic fragments are not exactly the same and, still more important, the existence of two

Table 1. ^{1}H NMR data for complexes **1–4** in acetone-d_6; allyl and *dppm* ligands[a]

Compound	Isomer	Allyl[b]					
		$H_{syn,\ cis}$	$H_{syn,\ trans}$	$H_{anti,\ cis}$	$H_{anti,\ trans}$	CH_3	CH_2-*dppm*
1 20°C	M	3.76 (m)	4.74 (m)	3.09 (s)	3.60 (m)	1.96	4.09 (t)
M/m = 55/45						(s)	$J_{HP} = 11.7$
	m	3.76 (m)	4.74 (m)	3.31 (s)	3.95 (m)	[c]	4.02 (t)
							$J_{HP} = 12.0$
2 −30°C	M	3.83 (m)	4.52 (pt)	3.33 (s)	3.72 (pt)	1.95	4.17 (t)
M/m = 58/42			$J_{HP} = 3.0$		$J_{HP} = 6.0$	(s)	$J_{HP} = 12.0$
	m	3.1 (m)	4.44 (pt)	2.41 (s)	2.72 (pt)	[c]	4.07 (t)
			$J_{HP} = 3.0$		$J_{HP} = 6.0$		$J_{HP} = 12.0$
3 0°C	M	3.68 (m)	3.91 (m)	2.98 (s)	3.53 (pt)	1.90	[c]
M/m = 57/43			$J_{HP} = 3.2$		$J_{HP} = 5.4$	(s)	
	m	3.76 (m)	3.97 (m)	3.22 (s)	3.76 (pt)	1.87	[c]
			$J_{HP} = 3.2$		$J_{HP} = 5.4$	(s)	
4 −40°C	M	4.07 (m)	4.30 (m)	3.21 (s)	3.77 (pt)	1.97	4.11 (t)
M/m = 52/48			$J_{HP} = 2.7$		$J_{HP} = 5.2$	(s)	$J_{HP} = 11.3$
	m	4.04 (m)	4.22 (m)	3.03 (s)	3.44 (pt)	2.02	4.04 (t)
			$J_{HP} = 3.0$		$J_{HP} = 5.1$	(s)	$J_{HP} = 11.5$

[a] Chemical shifts and coupling constants in ppm and Hz; M = major isomer, m = minor isomer, m = multiplet, s = singlet, pt = apparent triplet; see Experimental section for additional information; Ph-*dppm* groups appear in the range of 7.27–7.71 ppm; [b] *cis* and *trans* refers to the relative position of the terminal CH_2 allylic fragment with respect to the phosphorus atom of *dppm*; [c] not observed

Table 2. $^{13}C\{^{1}H\}$ NMR data for complexes **1–4** in acetone-d_6 at room temperature; allyl and *dppm* ligands[a]

Compound		Allyl[b]				
		CH_3	$CH_{2\ cis\ P}$	$CH_{2\ trans\ P}$	−C =	CH_2-*dppm*
1	M	23.17 (s)	61.72 (s)	80.49 (pt)	[c]	24.55 (t)
				$J_{CP} = 17.5$ Hz		$J_{CP} = 18.7$ Hz
	m	23.17 (s)	61.52 (s)	80.80 (pt)	[c]	24.62 (t)
				$J_{CP} = 15.7$ Hz		$J_{CP} = 19$ Hz
2	M	23.78 (s)	56.1 (s)	78.2 (m)	[c]	23.7 (m)
	m	23.35 (s)	57.5 (s)	78.5 (m)	[c]	25.2 (m)
3	M	23.2 (s)	65.8 (s)	78.17 (pt)	[c]	23.82 (t)
				$J_{CP} = 14.6$ Hz		$J_{CP} = 15$ Hz
	m	22.93 (s)	66.79 (s)	79.85 (pt)	[c]	25 (t)
				$J_{CP} = 15.1$ Hz		$J_{CP} = 16.1$ Hz
4		23.4 (s)	65.9 (s)	78 (pt)	140 (s)	23.7 (t)
				$J_{CP} = 12.5$ Hz		$J_{CP} = 18.7$ Hz

[a] Chemical shifts in ppm; M = major isomer, m = minor isomer, s = singlet, pt = apparent triplet, t = triplet; see Experimental section for additional information; Ph-*dppm* groups appear in the range of 128–136 ppm; [b] *cis* and *trans* refers to the relative position of the terminal CH_2 allylic group with respect to the phosphorus atom of *dppm*; [c] not observed

signals for the H_4 pyrazolic protons in **2** and also for H_5 of the pyridine group in **4** indicate the presence of two isomers. ^1H-^1H COSY spectra at low temperatures were used to correlate the signals of a given isomer and also to infer the position of some signals obscured by the solvent or the phenylic resonances in the corresponding monodimensional spectra.

The pyrazolate anion in **2** shows identical chemical shifts for H_3 and H_5 or C_3 and C_5 in each isomer; this is a consequence of their symmetrical arrangement in the molecules. The ^{19}F NMR spectra of the two isomers of **3** show the expected second-order patterns for the C_6F_5 group in a non-restricted rotation regime with unique resonances for the *ortho* and *meta* ^{19}F nuclei.

Similar conclusions regarding the presence of two isomers could also be drawn from the $^{13}C\{^1H\}$ NMR spectra that were recorded at room temperature. As in the $^{31}P\{^1H\}$ NMR spectra, only averaged signals were observed for **4** in the corresponding $^{13}C\{^1H\}$ NMR spectrum.

Assuming a boat conformation for the metallacycle formed in these complexes (confirmed by the X-ray diffraction studies), two relative orientations for the 2-Me-allyl groups (*i.e*. *cis* and *trans*) are possible (see Scheme 3). Considering the orientation of the allyl groups with respect to the metallacycle, two conformers could be formed in the *cis* case (*cis*-I and *cis*-II). These conformers could interconvert by a boat-to-boat inversion. When the two allyl groups are in a *trans* disposition, such an interconversion process would lead to the same conformer. The interconversion between the *cis* and *trans* forms would be possible by an apparent allyl rotation.

In order to obtain more information about the isomers present in solution, the appearance of the CH_2-*dppm* groups in the ^1H NMR spectra must also be considered. A triplet is observed for each isomer even at low temperature. This points to a boat-to-boat inversion process that exchanges the respective axial-equatorial position of the methylene protons and makes them equivalent in the local environment of the symmetric *dppm* coordinated ligand. In the case of the *cis*

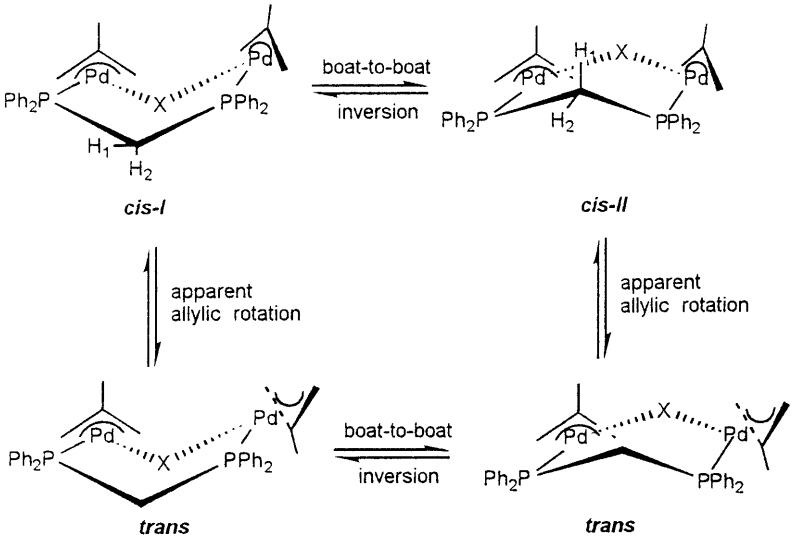

Scheme 3

isomer, the boat-to-boat inversion process alone could not account for the equivalence of these protons, but it is possible that the allyl groups are too remote to influence significantly the chemical shift and, as a consequence, both protons appear equivalent. The low barrier for this fluxional process contrasts with the observed rigidity of the same metallacycle in $[Pd_2(o\text{-}C_6H_4C{=}NC(H){=}C(H)CMe)_2(\mu\text{-}dppm)(\mu\text{-}Cl)]Cl$ [11]. In this example, an *o*-metallated 2-phenylimidazole replaces the allyl group of **1**–**4**. Consequently, and considering the interconversion between the *cis*-I and *cis*-II forms, the two species observed in solution must correspond to the *cis* and *trans* isomers (see Scheme 3). Thus, the observed isomerization process near room temperature must correspond to the apparent allyl rotation. Additional information about this process will be given below. Assignment of a particular structure (*cis* or *trans*) to a group of signals, *e.g.* to the major or minor isomer, was not possible due to the similar environment of all chemical groups in the two molecular forms. Besides, the two allyl groups are too far from each other for any NOE effects to be observed between their respective resonances.

Molecular structures of **2** and **4**

The molecular structures of compounds **2** and **4** were solved by X-ray diffraction studies. The X-ray crystallographic data are shown in Table 3, and the most significant intramolecular distances and bond angles, along with their standard deviations, are listed in Table 4.

Table 3. Crystallographic data and structure refinement details for **2** and **4**

	2 · $1/2C_2H_4Cl_2$	**4**
Empirical formula	$C_{38}H_{41}ClF_3N_2O_3P_2Pd_2S$	$C_{39}H_{40}F_3NO_3P_2Pd_2S_2$
Formula weight	972.98	966.58
Temperature/K	293(2)	293(2)
Wavelength/Å	0.71070	0.71070
Crystal system, space group	orthorhombic, $P2_12_12_1$	monoclinic, $P2_1/c$
a/Å	9.740(10)	15.296(2)
b/Å	20.7570(10)	12.3090(10)
c/Å	21.620(2)	22.044(9)
β/°		104.880(10)
Volume/Å^3	4371(5)	4011(2)
Z, Calculated density/g/cm^3	4,1.479	4, 1.601
Absorption coefficient/cm^{-1}	10.53	11.32
F(000)	1956	1944
Crystal size/mm	0.4×0.3×0.3	0.3×0.3×0.2
Limiting indices	$0 \le h \le 12$, $0 \le k \le 27$, $0 \le l \le 28$	$0 \le h \le 20$, $0 \le k \le 16$, $-29 \le l \le 28$
Data / restraints / parameters	5827 / 0 / 461	9661 / 0 / 421
Goodness-of-fit on F^2	1.050	0.969
Final *R* indices ($I > 2\square(I)$)	$R_1 = 0.0626$, $wR_2 = 0.1461$	$R_1 = 0.0537$, $wR_2 = 0.1530$
Absolute structure parameter	0.05(8)	
Largest diff. peak and hole/e · Å^3	0.878 and −0.582	1.217 and −1.656

$R_1 = \Sigma||F_o| - |F_c||/\Sigma|F_o|$; $wR_2 = (\Sigma(w(F_o^2 - F_c^2)^2)/\Sigma(w(F_o^2)^2))^{0.5}$

Table 4. Selected bond lengths (Å) and angles (°) for **2** and **4**

2 · $\frac{1}{2}C_2H_4Cl_2$			
Pd(1)-N(1)	2.10(1)	N(1)-Pd(1)-C(7)	98.3(5)
Pd(1)-C(5)	2.12(1)	C(d)-Pd(1)-C(7)	66.2(6)
Pd(1)-C(6)	2.17(1)	N(1)-Pd(1)-P(2)	87.2(3)
Pd(1)-C(7)	2.22(1)	N(2)-Pd(2)-C(10)	98.5(5)
Pd(1)-P(2)	2.309(3)	C(8)-Pd(2)-C(10)	667.0(7)
Pd(2)-N(2)	2.07(1)	N(2)-Pd(2)-P(1)	96.5(3)
Pd(2)-C(8)	2.15(1)	C(8)-Pd(2)-P(1)	98.3(5)
Pd(2)-C(9)	2.17(1)	C(4)-P(1)-Pd(2)	114.3(4)
Pd(2)-C(10)	2.19(1)	C(4)-P(2)-Pd(1)	108.8(4)
Pd(2)-P(1)	2.296(4)	N(2)-N(1)-Pd(1)	121.3(7)
Pd(1)-Pd(2)	3.495(2)	N(1)-N(2)-Pd(2)	120.2(7)
P(1)-C(4)	1.84(1)	P(1)-C(4)-P(2)	112.2(7)
P(2)-C(4)	1.84(1)	C(7)-C(6)-C(5)	117.1(15)
		C(8)-C(9)-C(10)	116.8(17)
4			
Pd(1)-C(43)	2.157(7)	C(42)-Pd(1)-C(44)	66.2(3)
Pd(1)-C(42)	2.160(7)	C(42)-Pd(1)-P(6)	95.9(2)
Pd(1)-C(44)	2.176(8)	C(44)-Pd(1)-S(3)	102.5(2)
Pd(1)-P(6)	2.304(2)	P(6)-Pd(1)-S(3)	95.31(6)
Pd(1)-S(3)	2.350(2)	C(38)-Pd(2)-C(39)	37.9(4)
Pd(1)-Pd(2)	3.2081(9)	C(38)-Pd(2)-C(40)	66.5(4)
Pd(2)-C(38)	2.129(8)	C(38)-Pd(2)-P(5)	101.2(3)
Pd(2)-C(39)	2.165(8)	C(40)-Pd(2)-S(3)	100.3(3)
Pd(2)-C(40)	2.176(7)	P(5)-Pd(2)-S(3)	91.93(6)
Pd(2)-P(5)	2.297(2)	Pd(1)-S(3)-Pd(2)	85.69(6)
Pd(2)-S(3)	2.368(2)	C(25)-P(5)-Pd(2)	110.4(2)
S(3)-C(7)	1.799(7)	P(6)-C(25)-P(5)	114.0(3)
P(5)-C(26)	1.828(7)	C(38)-C(39)-C(40)	116.3(9)
P(5)-C(32)	1.828(6)	C(44)-C(43)-C(42)	116.0(9)
P(5)-C(25)	1.853(7)		
P(6)-C(13)	1.815(6)		
P(6)-C(19)	1.806(7)		
P(6)-C(25)	1.837(7)		

Compound **2** can be crystallized from 1,2-dichloroethane/pentane to give well-formed colourless single crystals. The structure of **2** agrees with the proposed binuclear nature of the system. An ORTEP view of the cation together with the atom labelling scheme is shown in Fig. 1. The seven-membered $Pd_2P_2CN_2$ chelate ring shows a distorted boat conformation with a torsion angle P(1)-Pd(2)-Pd(1)-P(2) of $-18.31(5)°$. The pyrazolate ring points away from the metallacycle ring. The two N atoms form the stern of the boat. The two methyl groups of the allyl unit are orientated toward the same side of the metallacycle (*cis* isomer).

The dihedral angles between coordination (Pd(1)-P(2)-N(1) and Pd(2)-P(1)-N(2)) and allylic (C(5)-C(6)-C(7) and C(8)-C(9)-C(10)) planes for **2** amount to

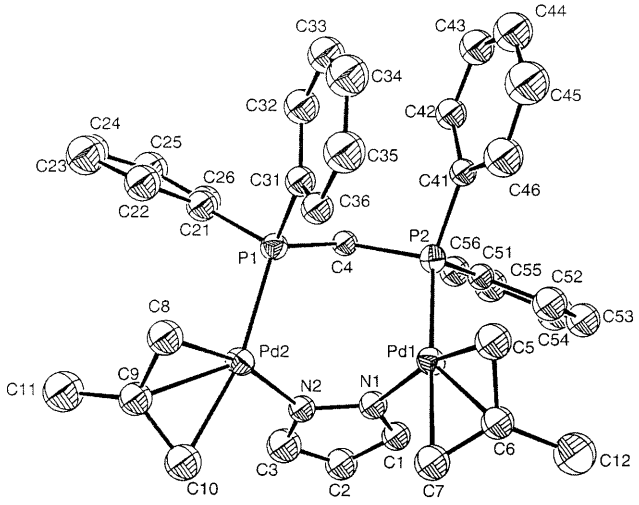

Fig. 1. Structure of $[Pd_2(\eta^3\text{-Me-}C_3H_4)_2(\mu\text{-}pz)(\mu\text{-}dppm)]Tf \cdot \frac{1}{2}CH_2ClCH_2Cl$ (**2** $\cdot \frac{1}{2}CH_2ClCH_2Cl$; the solvent and anion are omitted for clarity) showing 30% probability thermal ellipsoids

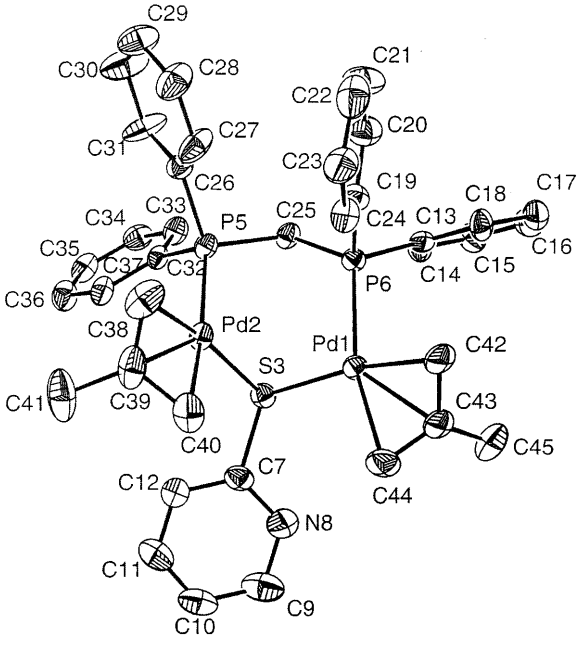

Fig. 2. Structure of $[Pd_2(\eta^3\text{-Me-}C_3H_4)_2(\mu\text{-S}py)(\mu\text{-}dppm)]Tf$ (**4**; the anion is omitted for clarity) showing 30% probability thermal ellipsoids

110(1) and 109.4(9)°. In the allyl ligands, the C(6)-C(12) and C(9)-C(11) vectors point away from the metal with C(11) and C(12) at distances of −0.22(2) and 0.26(2) Å outside of the respective allylic planes.

Compound **4** can be crystallized from 1,2-dichloroethane/ether to give well-formed orange single crystals. An ORTEP view of the cation together with the atom labelling scheme is shown in Fig. 2. The local coordination around each metal

centre is a distorted square-planar geometry with the P atom, the S atom, and the η^3-allyl ligand comprising the immediate coordination sphere. The coordination planes defined by Pd(1)-P(6)-S(3) and Pd(2)-P(5)-S(3) are approximately prependicular to the allyl ligand planes defined by C(42)-C(43)-C(44) and C(38)-C(39)-C(40), with dihedral angles of 110.7(6) and 113.3(5)°. In the allyl ligands, the C(39)-C(41) and C(43)-C(45) vectors point away from the metal. The atoms C(41) and C(45) are 0.31(1) and 0.18(1) Å outside of the respective allylic planes.

The six-membered Pd_2P_2CS chelate ring shows a distorted boat conformation. Palladium and phosphorus atoms are on the boat deck with a torsion angle P(5)-Pd(2)-Pd(1)-P(6) of 19.42(6)°. Sulfur and CH_2-groups constitute the bow and stern of the boat with a distorted tetrahedral sp^3-hybridized geometry. The Pd-Pd distance is long (3.2081(9) Å), and as a consequence the presence of a metal-metal bond can be excluded. This metallacycle ring has only one precedent in the literature in Pd(II) dinuclear complexes, *i.e.* $[Pd_2\ (o\text{-}C_6H_3(OMe)C{=}NCy)_2(\mu\text{-}(PPh_2)_2C{=}CH_2))(\mu\text{-}Cl)]Cl \cdot CHCl_3$ [12], whereas it has been more widely described in Pd(I) dinuclear complexes with metal-metal bonds [13]. As in **2**, the two methyl groups of the allyl moiety are orientated toward the same side of the metallacycle (*cis* isomer). The pyridine group is in an equatorial disposition on the metallacycle ring with minor steric hindrance.

Fluxional behaviour of complexes **2** and **4**

The fluxional behaviour of complexes **2** and **4** was studied both in acetone-d_6 and in 1,1′,2,2′-tetrachloroethane-d_2. These solvents were selected due to the difference in their coordination ability and to the temperature range of their liquid state, which allowed a complementary NMR study to be undertaken. The dynamic process involves the interconversion of the *cis* and *trans* stereoisomers. This fact was clearly indicated by the coalescence of the resonances of the two isomers for several chemical groups such as the CH_2-*dppm* protons, the allylic methyl groups, and the pyrazolic H_4 protons. In Table 5 the different $\Delta G_T^{\ddagger}$ values obtained at the coalescence temperature are given. In some cases, the data were not calculated because of some uncertainty in the determination of the coalescence temperature

Table 5. Calculated $\Delta G_T^{\ddagger}$ values from the coalescence temperatures for complexes **2** and **4** according to the *Eyring* expression [16]

Entry	Complex	Coalescing groups[a]	Solvent	T_c/K	$\Delta\nu$/Hz	$\Delta G_T^{\ddagger}$/ kJ · mol^{-1}
1	**2**	H_4	acetone-d_6	300	9.22	66.0
2	**2**	$H_{syn,\ trans}$	acetone-d_6	301	14.01	65.2
3	**2**	$H_{syn,\ trans}$	tetrachloroethane-d_2	388	16.39	84.2
4	**4**	$H_{syn,\ trans}$	tetrachloroethane-d_2	248	9.10	53.5
5	**4**	Me	tetrachloroethane-d_2	268	24.58	56.5
6	**4**	$H_{syn,\ trans}$	acetone-d_6	264	14.83	57.2
7	**4**	Me	acetone-d_6	263	6.77	58.2

[a] Refers to two similar groups of the major and minor stereoisomers

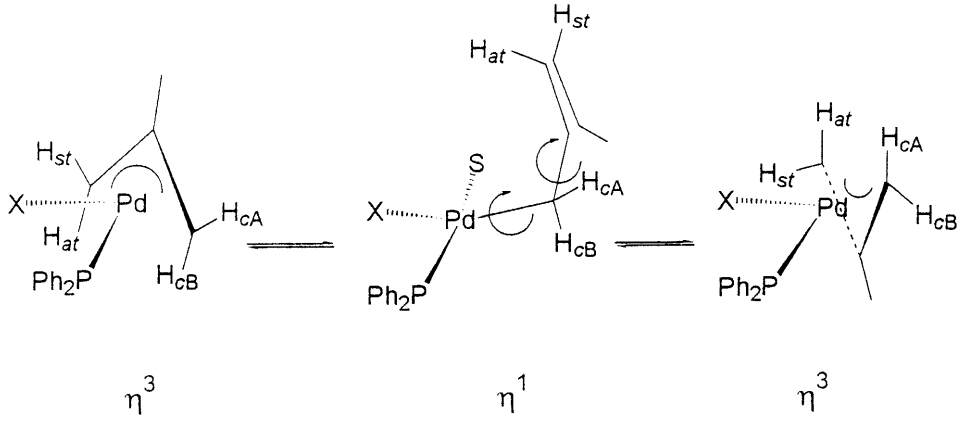

Scheme 4

due to signal overlap. With respect to the allylic groups, coalescence of the $H_{syn,\ trans}$ proton of one isomer with the $H_{syn,\ trans}$ proton of the other isomer was observed in every case (see Table 5). This coalescence takes place more easily than that for the corresponding $H_{syn,\ cis}$ protons. For example, in complex **2** (1,1′,2,2′-tetrachloroethane-d_2 solution), the $H_{syn,\ cis}$ protons, even though they have a smaller $\Delta\nu$ value, did not yet coalesce at the temperature at which coalescence of the $H_{syn,\ trans}$ protons had already taken place. After the coalescence of the signals for the $H_{syn,\ trans}$ protons the resuting singlet narrows, although it subsequently broadens in a similar way to the other allylic signals. In one case (complex **4** in 1,1′,2,2′-tetrachloroethane-d_2) we observed the appearance of two signals at high temperature after the complex process of the coalescences of the eight resonances. In this instance, although without quantitative data, it can also be seen that the coalescence of the signals of the *syn*, *cis* protons with those of the *anti*, *cis* protons is easier (higher $\Delta\nu$ and lower T_c) than the coalescence of the signals for *syn*, *trans* with the *anti*, *trans* protons. All these data point to a η^3-η^1-η^3 mechanism with the intermediate containing the η^1-allyl residue in *trans* position to N being probably more favourable than that with η^1-allyl trans to P (see Scheme 4). This process would lead to an inversion of the allyl group and consequently to an isomer interconversion and also to an interchange of the *syn* and *anti* protons at the carbon *cis* to phosphorus. If this selective mechanism were the only one operating, the *syn-anti* exchange would not take place in the protons *trans* to phosphorus. Examples of selective exchange in phosphine complexes have been described in the literature [14]. However, we do not have any data to exclude the same mechanism with transient decoordination of the carbon *cis* to phosphorus that would be of higher energy. The two narrowing signals observed at high temperature for complex **4** are due to the allylic protons *cis* or *trans* to phosphorus that do not interchange. This is an indication that a mechanism of *syn-syn*, *anti-anti* interchange is absent.

Comparison of entries 2 and 3 in Table 5 allows the evaluation of the influence of the solvent on the fluxional behaviour of complex **2**. For a similar $\Delta\nu$, in acetone-d_6 the T_c and also the $\Delta G_T^{\ddagger}$ values are clearly smaller, thus indicating a more facile process in this solvent. This could be due to the coordinating ability of acetone,

which could stabilize the intermediate formed in the mechanism proposed. A smaller solvent influence is observed for complex **4** (compare *e.g.* entry 6 with entry 5). However, a remarkable difference was found between complexes **2** and **4**. For example, comparison of entry 5 with entry 3 (same solvent) shows that for complex **2**, where $\Delta\nu$ is smaller than for complex **4**, T_c is by 80°C higher, and a big increase in the $\Delta G_T^{\ddagger}$ value is also observed. This implies that the isomer interconversion is a more facile process for complex **4**, probably through an intramolecular stabilization of the unsaturated intermediate in the proposed mechanism by the formation of Pd···N interactions. Such a situation would also explain the lower solvent effect for this complex as compared to **2**.

For complex **3**, an increase in the temperature to 323 K (acetone-d_6) does not produce any coalescence or broadening of the proton resonances. This lack of coalescence must be due to a large energy barrier, because there are signals of different isomers with a $\Delta\nu$ as low as 8 Hz. The same trend is observed in the ^{19}F NMR spectra. Consequently, there is no indication of isomer interconversion in this complex. A ^{19}F NMR study at low temperature (193 K) provides evidence of a free rotation situation for the pentafluorophenyl group even at this temperature.

Experimental

All manipulations were carried out under an atmosphere of dry oxygen-free nitrogen using standard *Schlenk* techniques. Solvents were distilled from the appropriate drying agents and degassed before use. $[Pd_2(\eta^3\text{-2-Me–}C_3H_4)_2(\mu\text{-Cl})_2]$ was prepared as described in the literature [15]. Elemental analyses were performed with a Perkin-Elmer 2400 micro analyser; the results agreed favourably with the calculated values. IR spectra were recorded as Nujol mulls with a Perkin-Elmer PE 883 IR spectrometer. ^1H, ^{13}C, ^{19}F, and ^{31}P NMR spectra were recorded on a VARIAN UNITY 300 spectrometer at 20°C. Chemical shifts (ppm) are given relative to *TMS* (^{13}C and ^1H), CF_3Cl (^{19}F), and 85% H_3PO_4 (^{31}P). COSY spectra: standard pulse sequence, acquisition time 0.214 s, pulse width 10 µs, relaxation delay 1 s, 16 scans, 512 increments. For variable temperature spectra the probe temperature (±1 K) was controlled by a standard thermocontrol unit calibrated with a methanol reference. Free energies of activation were calculated [16] from the coalescence temperature (T_c) and the frequency difference between the coalescing signals (extrapolated at the coalescence temperature) according to the formula $\Delta G_c^{\ddagger} = aT(9.972 + \log(T/\Delta\nu))$, $a = 1.914 \times 10^{-2}$. The estimated error in the calculated free energies of activation is $\pm 1.0\,kJ \cdot mol^{-1}$. The descriptors M and m refer to the major or minor isomers, respectively.

$[Pd_2(\eta^3\text{-}Me\text{-}C_3H_4)_2(\mu\text{-}Cl)(\mu\text{-}dppm)]Tf$ (**1**; $C_{34}H_{35}ClF_3O_3P_2Pd_2S$)

$AgCF_3SO_3$ (65 mg, 0.25 mmol) was added to a solution of $[Pd(\eta^3\text{-2-Me-}C_3H_4)(\mu\text{-Cl})]_2$ (100 mg, 0.25 mmol) in *THF* (30 cm^3). After 1 h of reaction the resulting yellow solution was filtered, and *dppm* was added (98 mg, 0.25 mmol). The resulting suspension became pale yellow and was stirred for 12 h. This solution was evaporated up to 3 cm^3, and diethyl ether was added. A white solid was obtained which was filtered and dried under vacuum.

Yield: 209.4 mg (94%); IR: 228 and 250 cm^{-1} (ν(Pd-Cl)); ^{31}P NMR (acetone-d_6, 121.4 MHz): $\delta = 20.24$ (2P, $dppm_m$), 20.40 (2P, $dppm_M$) ppm.

$[Pd_2(\eta^3\text{-}Me\text{-}C_3H_4)_2(\mu\text{-}pz)(\mu\text{-}dppm)]Tf$ (**2**; $C_{37}H_{38}F_3N_2O_3P_2Pd_2S \cdot C_2H_4Cl_2$)

To a solution of Na*pz* prepared by mixing NaH (4.5 mg, 0.11 mmol), previously washed with hexane, and *pz*H (7.7 mg, 0.11 mmol) in 35 cm^3 of *THF*, 100 mg (0.11 mmol) **1** were added. After 24 h of

stirring, a colourless suspension was obtained. The precipitated salt was filtered, and the solution was evaporated to dryness. The resulting solid was washed with diethyl ether ($2 \times 3\,cm^3$) and dried under vacuum.

Yield: 99 mg (88%); IR: $1580\,cm^{-1}$ (ν(CN) of *pz* [18]); ^1H NMR (acetone-d_6, 300 MHz): 6.22 (t, $^3J_{HH} = 2.0$ Hz, 1H, H_m^4, *pz*), 6.27 (t, $^3J_{HH} = 2.0$ Hz, 1H, H_M^4, *pz*), 7.08 (t, $^3J_{HH} = 2.0$ Hz, 2H, H_m^{3+5}, *pz*), 7.48 (t, $^3J_{HH} = 2.0$ Hz, 2H, H_M^{3+5}, *pz*) ppm; $^{13}C\{^1H\}$ NMR (acetone-d_6, 75 MHz): 106.2 (2C, C_{m+M}^4, *pz*), 143.1 (2C, C_m^{3+5}, *pz*), 144.0 (2C, C_M^{3+5}, *pz*) ppm; ^{31}P NMR (acetone-d_6, 121.4 MHz): 23.97 (2P, $dppm_M$), 26.45 (2P, $dppm_m$) ppm.

[$Pd_2(\eta^3$-Me-$C_3H_4)_2(\mu$-$SC_6F_5)(\mu$-dppm)]Tf (**3**; $C_{40}H_{35}F_8O_3P_2Pd_2S_2$)

150 mg (0.17 mmol) of **1** and 68 mg (0.17 mmol) of $TlSC_6F_5$ were added to $30\,cm^3$ of acetone. After 24 h of stirring, an orange suspension was obtained. The TlCl was filtered, and the solution was evaporated to dryness. The resulting solid was washed with diethy ether ($2 \times 3\,cm^3$) and dried under vacuum.

Yield: 145.2 mg (81%); IR: 1508, 1077, 975 and $786\,cm^{-1}$ ($\nu(C_6F_5)$ [19]); $^{13}C\{^1H\}$ NMR (acetone-d_6, 75 MHz): 120.9 (q, $^1J_{CF} = 320$ Hz, 1C, CF_3SO_3), 137.7 (bd, $^1J_{CF} = 255$ Hz, 2C, C^{meta}, C_6F_5), 146.2 (bd, $^1J_{CF} = 248$ Hz, 2C, C^{ortho}, C_6F_5) ppm; ^{19}F NMR (acetone-d_6, 282.2 MHz): −79.23 (s, 3F, CF_3SO_3), −130.89 (m, 2F, F_m^{ortho}, C_6F_5), −131.22 (m, 2F, F_M^{ortho}, C_6F_5), −157.58 (t, $^1J_{FF} = 21.4$, 1F, F_m^{para}, C_6F_5), −158.55 (t, $^1J_{FF} = 21.4$, 1F, F_M^{para}, C_6F_5), −162.34 (m, 2F, F_m^{meta}, C_6F_5), −163.00 (m, 2F, F_M^{meta}, C_6F_5) ppm; ^{31}P NMR (acetone-d_6, 121.4 MHz): 16.04 (2P, $dppm_m$), 16.54 (2P, $dppm_M$) ppm.

*[$Pd_2(\eta^3$-Me-$C_3H_4)_2(\mu$-S*py*$)(\mu$-dppm)]Tf* (**4**; $C_{39}H_{39}F_3NO_3P_2Pd_2S_2$)

100 mg (0.11 mmol) of **1** and 16 mg (0.11 mmol) of KS*py* (prepared from KOH and HS*py* in methanol [17]) were added to $30\,cm^3$ of *THF*. After stirring for 4 h, an orange suspension was obtained. The KCl was filtered, and the solution was evaporated to dryness. The resulting solid was washed with diethyl ether ($2 \times 3\,cm^3$) and dried under vacuum.

Yield: 92.4 mg (87%); IR: $1540\,cm^{-1}$ (ν(CN) of pyridine [20]); ^1H NMR (acetone-d_6, 300 MHz): 7.19 (d, $^3J_{HH} = 4.5$ Hz, 1H, H_m^5, S*py*), 7.21 (d, $^3J_{HH} = 5.1$ Hz, 1H, H_M^5, S*py*), 8.42 (m, 2H, H_{m+M}^6, S*py*) ppm; $^{13}C\{^1H\}$ NMR (acetone-d_6, 75 MHz): 121.8 (1C, C^4, S*py*), 128.0 (1C, C^3, S*py*), 136.7 (1C, C^5, S*py*), 149.3 (1C, C^6, S*py*), 164.0 (1C, C^2, S*py*) ppm; ^{31}P NMR (acetone-d_6, 121.4 MHz): 20.07 (2P, *dppm*) ppm.

X-Ray structure determination of **2** and **4**

Crystal, data collection, and refinement parameters are collected in Table 3. Suitable crystals were selected and mounted on fine glass fibers with epoxy cement. The unit cell parameters were determined from the angular setting of a least-squares fit of 25 strong high-angle reflections. Reflections were collected at 25°C on a NONIUS-MACH3 diffractometer equipped with a graphite monochromated radiation ($\lambda = 0.71070$ Å). None of the samples showed significant intensity decay over duration of data collection.

Data were corrected in the usual fashion for *Lorentz* and polarization effects; correction for the empirical absorption was not necessary ($\mu = 10.53\,cm^{-1}$ (**2**) and $11.32\,cm^{-1}$ (**4**)). The space group was determined from the systematic absences in the diffraction data. The structures were solved by direct methods [21], and refinements on F^2 were carried out by full-matrix least squares analysis [22].

Anisotropic temperature parameters were considered for all non-hydrogen atoms, except the triflate and dichloroethane groups, whereas hydrogen atoms were included in calculated position but

not refined. For the disordered CF_3SO_3 in both compounds, occupancies were refined initially and then fixed. Selected bond parameters are collected in Table 4.

Crystallographic data have been deposited at the Cambridge Crystallographic Data Center (CCDC 145409 and CCDC 145410 for **2** and **4**, respectively).

Acknowledgements

We gratefully acknowledge financial support from the *Dirección General de Investigación Científica y Técnica* (*DGICyT*) (Grant No. PB98-0315) of Spain.

References

[1] (a) Barnard CFJ, Russell JH (1987) In: Wilkinson G (ed) Comprehensive Coordination Chemistry, vol 5. Pergamon Press, Oxford, p 1099; (b) Roundhill DM (1987) ibid, p 351
[2] a) Powel J, Shaw BL (1968) J Chem Soc A 774; b) Pringle GP, Shaw BL (1983) J Chem Soc Dalton Trans 889; c) Issleib K, Abicht HP, Winkelmann HZ (1972) Anorg Allg Chem **89**: 388; d) Kluwe C, Müller J, Davies JA (1996) J Organomet Chem **526**: 385; e) Davies JA, Pinkerton AA, Syed R, Vilmer R (1988) J Chem Soc Chem Commun 47; f) Kluwe C, Davies JA (1995) Organometallics **14**: 4257; g) Klopfensstein SR, Kluwe C, Krischbaum K, Davies JA (1996) Can J Chem **74**: 2331
[3] Benner SL, Olmstead MM, Hope H, Balch AL (1978) J Organomet Chem **153**: C31
[4] Benner LS, Balch AL (1978) J Am Chem Soc **100**: 6099
[5] Olmstead MM, Hope H, Benner LS, Balch AL (1977) J Am Chem Soc **99**: 5502
[6] Rattray AD, Sutton D (1978) Inorg Chim Acta **27**: L-85
[7] a) Balch AL, Hunt CT, Lee CL, Olmstead MM, Farn JP (1981) J Am Chem Soc **103**: 3764; b) Kubiak CP, Eisenberg R (1977) J Am Chem Soc **99**: 6129
[8] Hassan FSM, Markham DP, Pringle PG, Shaw BL (1984) J Chem Soc Dalton Trans 279
[9] Nakamoto K (1986) Infrared and Raman Spectra of Inorganic and Coordination Compounds. Wiley, New York
[10] a) Wilkinson G, Stone GA, Abel EW (1982) Comprehensive Organomet Chem, vol 6. Pergamon Press, Oxford; b) Kurosawa H, Asada N (1983) Organometallics **2**: 251; c) Fernández-Galán R, Manzano BR, Otero A (1999) J Organomet Chem **577**: 271; d) Fernández-Galán R, Jalón FA, Manzano BR, Rodríguez-de la Fuente J, Vrahami M, Jedlicka B, Weissensteiner W, Jogl G (1997) Organometallics **16**: 3758
[11] Vila JM, Gayoso M, Pereira MT, Ortigueira JM, López-Torres M, Castiñeiras A, Suárez A, Fernández JJ, Fernández A (1997) J Organomet Chem **547**: 297
[12] Vila JM, Ortigueira JM, Gayoso E, Gayoso M, Castiñeiras A, Hiller W, Strahle J (1991) Inorg Chim Acta **179**: 171
[13] a) Usón R, Forniés J, Sanz JF, Usón MA, Usón I, Herrero S (1977) Inorg Chem **36**; 1912; b) Leoni P, Pasquali M, Pieri G, Englert U (1996) J Organomet Chem **514**: 243
[14] a) Breutel C, Pregosin PS, Salzmann R, Togni A (1994) J Am Chem Soc **116**: 4067; b) Pregosin PS, Salzmann R, Togni A (1995) Organometallics **14**: 842; c) Pregosin PS, Salzmann R (1996) Coord Chem Rev **155**: 35; d) Hosocawa T, Wakabayashi Y, Hosokawa K, Tsuji T, Murahashi SI (1996) J Chem Soc Chem Commun 859; e) Fernández-Galán R, Jalón FA, Manzano BR, Rodríguez-de la Fuente J, Vrahami M, Jedlicka B, Weissensteiner W (1997) Organometallics **16**: 3758
[15] a) Dent WT, Long R, Wilkinson G (1964) J Chem Soc 1585; b) Tatsuno Y, Yoshida T, Seiotsuha (1979) Inorg Synth **19**: 220
[16] Sandström J (1982) Dynamic NMR Spectroscopy. Academic Press, London
[17] King RB, Welcman N (1969) Inorg Chem **8**: 2540

[18] Katritzky AR, Taylor PJ (1971) Phys Meth Hetrocycl Chem **4**: 265
[19] a) Long DA, Steele D (1963) Spectrochim Acta **19**: 1955; b) Deacon GB, Green JHS (1968) Spectrochim Acta **24**: 1125
[20] Katritzky AR, Topsom RD (1977) Chem Rev **77**: 639
[21] Altomare A, Cascarano G, Giacovazzo C, Guagliardi A, Burla MC, Polidori G, Camalli M (1994) J Appl Cryst 435
[22] Sheldrick GM (1997) Program for the Refinement of Crystal Structures from Diffraction data. University of Göttingen, Germany

Received June 7, 2000. Accepted June 20, 2000